PROGRESS IN PHOTOVOLTAICS: RESEARCH AND APPLICATIONS
Prog. Photovolt: Res. Appl. 2012; **20**:512–519
Published online 2 February 2012 in Wiley Online Library (wileyonlinelibrary.com). DOI: 10.1002/pip.2156

SPECIAL ISSUE: ADVENTURES IN CU-CHALCOGENIDE SOLAR CELLS

Kesterites—a challenging material for solar cells

Susanne Siebentritt[1]* and Susan Schorr[2]

[1] Laboratory for Photovoltaics, University of Luxembourg, Luxembourg
[2] Helmholtz-Zentrum Berlin für Materialien und Energie, Berlin, Germany

ABSTRACT

Kesterite materials ($Cu_2ZnSn(S,Se)_4$) are made from non-toxic, earth-abundant and low-cost raw materials. We summarise here the structural and electronic material data relevant for the solar cells. The equilibrium structure of both Cu_2ZnSnS_4 and $Cu_2ZnSnSe_4$ is the kesterite structure. However, the stannite structure has only a slightly lower binding energy. Because the band gap of the stannite is predicted to be about 100 meV lower than the kesterite band gap, any admixture of stannite will hurt the solar cells. The band gaps of Cu_2ZnSnS_4 and $Cu_2ZnSnSe_4$ are 1.5 and 1.0 eV, respectively. Hardly any experiments on defects are available. Theoretically, the Cu_{Zn} antisite acceptor is predicted as the most probable defect. The existence region of the kesterite phase is smaller compared with that of chalcopyrites. This makes secondary phases a serious challenge in the development of solar cells. Copyright © 2012 John Wiley & Sons, Ltd.

KEYWORDS
kesterite; CZTS; electronic structure; crystal structure; solar cell; defects; secondary phases

***Correspondence**
Susanne Siebentritt, Laboratory for Photovoltaics, University of Luxembourg, Luxembourg.
E-mail: susanne.siebentritt@uni.lu
Dedicated to Prof. Hans-Werner Schock on the occasion of his 65th birthday.

Received 23 September 2011; Revised 20 November 2011; Accepted 1 December 2011

1. WHY KESTERITES

Kesterites ($Cu_2ZnSn(S,Se)_4$) are attractive materials for absorbers in thin film solar cells. Currently, the best performing thin film solar cells on the cell as well as on the module level are based on chalcopyrite ($Cu(In,Ga)Se_2$) absorbers [1]. There are however concerns about indium. Both indium and gallium are rather costly metals, about 100 times more expensive than Cu and Zn (Table I). Photovoltaics is in competition with other industries, mainly the display industry for In and high speed semiconductor logics and optoelectronics for Ga. It should, however, be taken into account that the raw material prices make up only a relatively small part of the module production cost. Another concern is the availability of In, which might not be enough to produce solar cells on the terawatt per annum level [2]. This is clearly not a problem for today's chalcopyrite solar module industry, but maybe it is time now to study new materials to have them available when limitations to In supply become noticeable. The advantage of the kesterite materials is that they are isoelectronic to chalcopyrites, meaning that a number of their material properties, such as the crystal structure are very similar to chalcopyrites [3]. Also, the same preparation methods can be used and solar cells have been successfully prepared using the same device structure as chalcopyrite solar cells, making it an ideal alternative to In-containing absorbers. The elements in $Cu_2ZnSn(S,Se)_4$, besides Se, are all earth abundant with a high concentration in the crust (Table I). Solar cells based on $Cu_2ZnSn(S,Se)_4$ have achieved efficiencies above 10% [4]. The development and the challenges of kesterite solar cells have been recently reviewed [5,6]. Therefore, we concentrate in this review on the challenges concerning the material and its interfaces. Until recently, a number of very basic material properties have been disputed: it was not clear whether the structure is actually a kesterite structure [7] or a stannite structure [8,9], and the band gap of $Cu_2ZnSnSe_4$ had been reported between 0.8 [10] and 1.65 eV[11].

2. CRYSTAL STRUCTURE

The kesterite (space group $I\bar{4}$) and the stannite (space group $I\bar{4}2m$) structure differ in the ordering of Cu and Zn (Figure 1). When comparing the available International Council on Diffraction Data (ICDD) data on X-ray diffraction on Cu_2ZnSnS_4 and $Cu_2ZnSnSe_4$, it appears that the

Table I. Price and abundance of metals used in Cu chalcogenide solar cells.

Metal	Price ($/kg)*	Crust abundance ppb by weight**
Zn	2	79 000
Cu	9	68 000
Sn	27	2200
In	670	160
Ga	800	19 000

*Average prices for the last 12 months taken from www.metalprices.com and www.minormetals.com, data downloaded in August 2011.
**From www.webelements.com.

sulphide compound tends to appear in kesterite structure, whereas the selenide compound occurs in stannite structure. However because Cu^{+} and Zn^{2+} are isoelectronic, X-ray diffraction cannot distinguish between kesterite and stannite structure, because X-rays interact with the electron shell of the atoms. On the other hand, neutrons interact with the nuclei and can distinguish between Cu and Zn atoms [12]. In a comprehensive neutron diffraction study of various $Cu_2ZnSn(S,Se)_4$ compounds, it was shown that the sulphide as well as the selenide occur in the kesterite structure, not in the stannite structure. Both show a certain disorder in between the Cu and Zn sites [12].

Different polymorphs have also been observed in chalcopyrites: $CuInS_2$ occurs in the chalcopyrite structure as well as in CuAu ordering [13,14], whereas $Cu(In,Ga)Se_2$ is always in the chalcopyrite phase. This can be understood when looking at the differences in binding energies, which can be calculated by density functional theory: the binding energy of the chalcopyrite phase compared with the CuAu phase is 2 meV/atom larger for $CuInS_2$ and $CuInSe_2$, whereas it is 9 meV/atom larger for $CuGaSe_2$ [15]. Thus, the chalcopyrite phase is stabilised in $Cu(In,Ga)Se_2$ by the Ga addition, whereas in $Cu(In,Ga)S_2$ the polymorphism exists and has been shown to negatively influence the efficiency of solar cells [16]. This negative influence can—at least partly—be due to a smaller band gap of the CuAu phase [15].

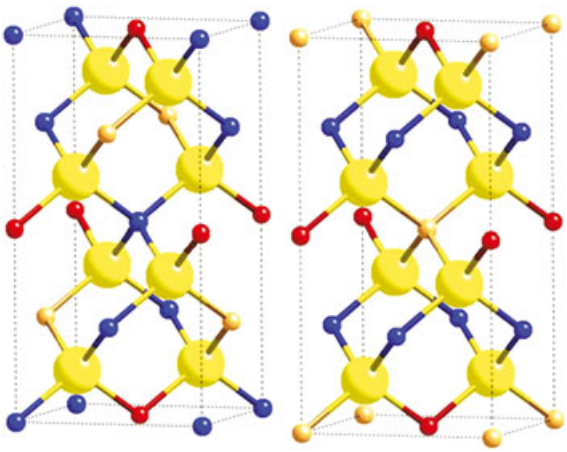

Figure 1. Kesterite (left) and stannite (right) structure; large yellow spheres: S and Se; small spheres: blue, Cu; yellow, Zn; red, Sn. Taken from [12].

The binding energies of the kesterite versus the stannite phase in $Cu_2ZnSn(S,Se)_4$ have been calculated by several groups using density functional theory [17–20] or hybrid functionals [19]. They are summarised in Table II. All recent calculations find a few millielectron volts per atom lower binding energy for the stannite compared with the kesterite.

Earlier work found a difference of around −10 meV [17], but it is unclear from the paper whether this is per atom or per unit cell. One thing becomes clear: all calculations predict the kesterite as the most stable phase for the sulphide and the selenide. However, the energy difference of the stannite structure is only slightly larger than the energy difference of the CuAu ordering in $CuInS_2$. It is therefore likely that stannite coexists with kesterite, which explains the disorder between Cu and Zn sites found experimentally [12]. Because the band gaps predicted for the stannite structure are smaller than those of the kesterite, this could be one reason for the relatively low open-circuit voltages observed in kesterite solar cells compared with the band gap [5,6]. The stability of CuAu ordering in the kesterite system has also been studied, usually the energy difference with respect to the kesterite phase is very similar to the energy difference of the stannite with respect to the kesterite [18]; however, Paier *et al*. found a considerably lower energy difference in the case of CuAu ordering than in the case of stannite [19].

Another structural parameter with important consequences for the electronic structure is the tetragonal distortion, which also occurs in chalcopyrites, i.e. the deviation of the ratio of the long axis c over two times the short axis from 1: $c/2a \neq 1$. This deviation leads to a crystal field and to a non-degenerate valence band maximum [21]. The sign of the crystal field is important for the symmetry of the topmost valence band [21–23], which in turn is critical for the anisotropy of the effective mass [24]. Therefore, it is important to look into the $c/2a$ values found experimentally and theoretically.

A combination of X-ray and neutron powder diffraction found a $c/2a$ value in Cu_2ZnSnS_4 powder samples of just very slightly above 1, namely 1.0008 [25]. A dependence of the a lattice constant and of the $c/2a$ ratio on the cooling rate during crystal growth was found. A detailed investigation of non-stoichiometric polycrystalline thin films by grazing incidence X-ray diffraction indicates a $c/2a < 1$. This is summarised in Figure 2.

The powder samples are grown by solid state synthesis [25], the thin film from HZB is grown by a coevaporation

Table II. Difference in binding energy of the stannite with respect to the kesterite phase calculated by several authors and given in meV/atom.

	Chen *et al.* [18]	Paier *et al.* [19]	Persson [20]
Selenide	−3.8		−3.3
Sulphide	−2.9	−2.9…−3.4	−1.3

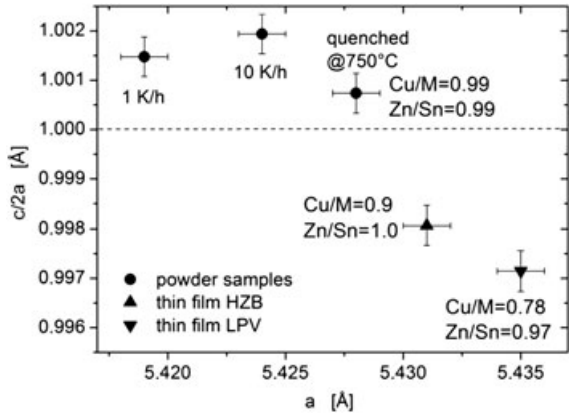

Figure 2. Lattice parameters determined by X-ray and neutron diffraction on powder samples and two different thin films of Cu_2ZnSnS_4. For the powder samples, the cooling rates during the synthesis are given as well as for all samples the chemical composition in terms of the Cu/M (M = Zn + Sn) and Zn/Sn ratios.

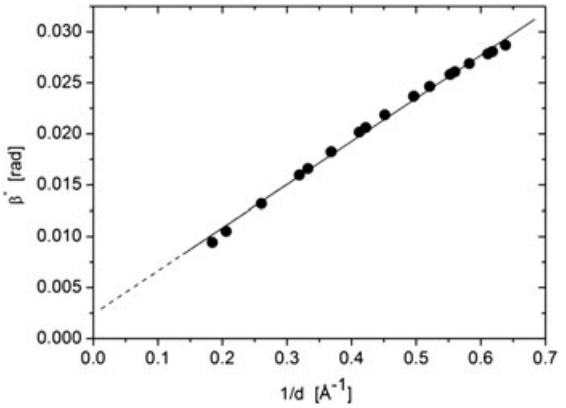

Figure 3. Williamson–Hall plot for a CZTS thin film ($\beta^* = \beta \cdot (\cos(\theta)/\lambda)$ where θ is the position of the Bragg peak in the diffraction pattern and λ is the X-ray wave length).

process using ZnS, Cu, Sn and S sources [26], and the thin film from LPV is grown by electrodeposition of metallic precursors followed by annealing, as described in [27]. All single crystals show a $c/2a > 1$. The sample with the slowest cooling is expected to be closest to equilibrium. From this we conclude a $c/2a$ ratio of 1.0015. The $c/2a$ ratios of the thin films are lower than 1. This can be attributed to strain and to the presence of secondary phases, because the thin films are less stoichiometric than the powder samples (labels in Figure 2). Nevertheless, this is significant because it shows that thin films might have a different effective mass than the bulk material, because of their different tetragonal distortion.

The existence of strain in CZTS polycrystalline thin films was identified in the sample grown at the HZB by applying the Williamson–Hall plot method [28]. In general the Williamson–Hall plot presents increasing strain by a steeper slope of the integral breadth β (which is obtained from the full width half maximum of the Bragg peaks) and the coherent domain size by the altitude at d equal to zero (d is the lattice plane distance). Figure 3 shows the Williamson–Hall plot for the polycrystalline CZTS thin film grown in the HZB. The slope indicates the existence of strain within the thin film.

For the selenide kesterites, a comparison of all the available ICDD data gives a $c/2a$ ratio of just slightly <1. Two single crystals of $Cu_2ZnSnSe_4$ were grown by the Bridgeman method. No. 1 is grown by direct reaction of a stoichiometric mixture of Cu, Zn, Sn and Se which was placed in an 18-mm-diameter quartz ampoule covered inside with graphite. The sealed ampoule was quickly heated to 600°C and kept at 600°C for 48 h. Then a heating step followed (rate of 10K/h to 950°C), this temperature was kept during 10–12 h. The ampoule was cooled to ~600°C with a rate of 10K/h. The next cooling step from 600°C to room temperature was made in switch off furnace mode. No. 2 was grown from an alloy of Cu, Zn and Sn, heated up to 850°C, holding the temperature for 72 h and cooling down with 21K/h. Both samples were slightly off-stoichiometric (no. 1: Cu/M = 1.03 and Zn/Sn = 1.07; no. 2: Cu/M = 1.05 and Zn/Sn = 1.03 as determined by electron microprobe analysis) and showed a complete disorder of Cu and Zn on the 2*c* and 2*d* Wyckoff sites (concerning kesterite type structure) [29]. The *a* lattice parameters of both $Cu_2ZnSnSe_4$ samples determined by simultaneous refinement of X-ray and neutron diffraction are very similar—0.5697(2) and 0.5693(2) nm—the $c/2a$ ratio is in both cases 0.9960(4). The most plausible equilibrium lattice parameters extracted from these investigations are summarised in Table III.

Structures have also been calculated [17–20]. The studies in [17,18] and [20] agree that the lattice parameters are smaller in the sulphide than in the selenide. All calculations [17–20] find a small tetragonal distortion: $0.998 \leq c/2a \geq 1.006$. However, on the trends between sulphide and selenide and between kesterite and stannite, there is no agreement between the different methods. Using the experimental values of Table III, which are based on a dedicated and comprehensive study, might help to improve the calculations.

3. ELECTRONIC BAND STRUCTURE

For a material to be used in solar cells, the electronic structure is of utmost importance: the band gap, the density of states, the doping behaviour and the transport properties.

Table III. Experimental lattice parameters and band gaps for Cu_2ZnSnS_4 and $Cu_2ZnSnSe_4$.

	a/Å	c/Å	c/2a	Eg/eV
Selenide	5.695	11.345	0.9960	1.0
Sulphide	5.419	10.854	1.0015	1.5

The following two sections discuss what is known about $Cu_2ZnSn(S,Se)_4$ in terms of electronic structure.

The band gap is experimentally determined by optical transmission measurements or by quantum efficiency measurements in solar cells. The vast majority of investigations finds the band gap of Cu_2ZnSnS_4 very close to 1.5 ± 0.01 eV [10,30–36]. For a long time, there has been quite a large range of reported band gaps from 0.8 [10] to 1.65 eV [11] for the selenide compound [10,11,37–41]. However, all measurements on $Cu_2ZnSnSe_4$ solar cells [10,40,41] showed band gaps around 1 eV. The discrepancy was recently solved by [42] who pointed out that the admixture of a ZnSe secondary phase caused the high band gaps determined by transmission measurements in the past and that the band gap of $Cu_2ZnSnSe_4$ is very close to 1.0 ± 0.01 eV. The values are added in Table III.

Density functional theory calculations in different approximations [17–20,43,44], hybrid functionals [18,19,43] and GW calculations [43] were applied to determine the band gap of $Cu_2ZnSn(S,Se)_4$ theoretically. All recent calculations for the kesterite structure agree quite well with the experimental band gaps, whereas the band gaps in stannite structure are about 100 meV lower. They are summarised in Table IV.

It is interesting to note that the low-temperature photoluminescence (PL) results are reported with two different peak energies for both materials. The peak energies cannot directly be compared with the band gap values: the PL measurements are performed at low temperatures, where the band gap is higher than at room temperature. In addition, all the PL peaks are broad and asymmetric and show large blue shifts with excitation density, which indicates the presence of fluctuating potentials [45,46] and shifts the emission peak to lower energies. However, these peaks can still be used as an indication for the band gap. These broad peaks have been found in the selenide compound at 0.85 [40] and 0.95 eV [47,48] and in the sulphide compound around 1.2 [49–51] and 1.3 eV [40,52,53]. One could assume that those samples showing the lower energy PL are dominated by the stannite structure, whereas samples with the higher energy PL peak are composed mostly of kesterite phase. It can also be speculated that the strong tailing observed in the quantum efficiency spectra of even the best solar cells [6,26,41,54–56] is due to the presence of a stannite phase with a lower band gap. Phase inhomogeneity with different band gaps is certainly detrimental to the solar cell efficiency, particularly to the open-circuit voltage [57].

Table IV. Calculated band gaps in eV for $Cu_2ZnSn(S,Se)_4$.

	Chen *et al.* [18]	Paier *et al.* [19]*	Persson [20]	Botti *et al.* [43]**
Se kesterite	0.96		1.05	1.02
Se stannite	0.82		0.89	0.87
S kesterite	1.50	1.49	1.56	1.64
S stannite	1.38	1.30	1.42	1.33

*Here we cite the hybrid functional results, which are expected to give the better description of the electronic structure.

**Here we cite the GW results, which are supposed to give the most accurate description of the electronic structure.

The calculations find a rather peculiar density of states in the conduction band [18–20,43]: the bottom of the conduction band is made of a lone band originating from the Sn-s and the S or Se-p states. This band is about 1 eV wide. At higher energies there is another gap within the conduction band, also approximately 1 eV wide. This gap is predicted to lead to a dip in the absorption spectrum [20]. This dip is currently not seen in quantum efficiency spectra, because its energy is beyond the band gap of CdS which is used as a buffer. However, when buffers with higher band gap will be used, this peculiarity of the density of states will lead to a loss in short-circuit current.

4. DEFECTS

Defects control the doping and thus the band bending as well as the recombination properties in solar cells. The related chalcopyrites are doped by intrinsic defects; so far, there is no indication that this is different in kesterites. Very limited experimental data are available on defects in kesterite. Defects in general are investigated by low temperature PL, admittance spectroscopy or electron spin resonance (EPR). No admittance investigations on kesterites have been published up to date. EPR investigations have found only broad peaks related to Cu(II) [8,58], very similar to the observations in chalcopyrites [59–61]. This makes EPR not useful for defect studies in these materials.

Most PL studies available show a broad peak, indicating fluctuating potentials. In this case, the PL emission is shifted in energy and it is not possible to extract defect data from such measurements. For defect spectroscopy, it is necessary to have narrow peaks that can be associated with donor–acceptor pair (DA) transitions or free to bound transitions [45]. There are only three reports of narrow peaks in PL measurements. All three were measured on Cu-rich samples, films or crystals [62–64]. This is an amazing parallel to the low temperature PL of chalcopyrite materials, where narrow emissions suitable for defect spectroscopy are only observed in Cu-rich material, whereas Cu-poor material shows broad luminescence indicative of fluctuating potentials [65–67]. In Cu-rich sulphide kesterite films or crystals, a DA transition at 1.496 eV was observed and an exciton at 1.509 eV [62], meaning that the defects involved in the DA transition must be rather shallow, 10 meV or less. Whether the second DA transition reported in [62] is in fact due to the kesterite material is disputed. A DA transition at 1.45 eV was also reported but not discussed in terms of involved defects [63]. In selenide kesterite material, an exciton at 1.033 eV has been observed, together with a DA transition

at 0.989 eV with two phonon replicas [64]. This has been interpreted as involving a donor at 7 meV below the conduction band and an acceptor at 27 meV above the valence band. A remarkable feature of both PL investigations [62,64] that found an exciton is that the excitonic emission quenches very fast and is not visible anymore above 20K.

A few theoretical studies on defects in kesterites are available [68–73], all based on density functional theory, which has its limitations predicting defect levels [43,74]. However, defect formation energies can be considered correct. Defect formation energies depend on composition and on the Fermi level. Nevertheless, some general trends can be extracted. The investigations agree that the defect with the lowest energy of formation, under many conditions even negative, is the Cu_{Zn} antisite defect and it is an acceptor. Generally, the donor defects have higher formation energies, most likely donors according to [71,75] are the S vacancy and the Zn_{Cu} antisite. Further low formation energy acceptors are the Cu_{Sn} antisite and the Cu vacancy. The low, often negative formation energy of the most probable acceptor, namely the Cu_{Zn} antisite, can explain that Cu_2ZnSnS_4 [10,31,36,51,76–80] and $Cu_2ZnSnSe_4$ [37–39,81] have always been found as p-type. There are no reports on n-type $Cu_2ZnSn(S,Se)_4$ material. It can be assumed that the p-type character is due to the Cu_{Zn} or Cu_{Sn} antisites and the Cu vacancy, with compensation from the Zn_{Cu} antisite and the S vacancy. Most available low-temperature PL investigations show broad asymmetric emissions [40,47–53,82] indicating that the material is in fact strongly compensated.

5. SECONDARY PHASES

The previous sections discuss the challenges related with the kesterite material itself. However, it is even a challenge to prepare $Cu_2ZnSn(S,Se)_4$ single phase. Because it is a truly quaternary crystal, a large number of secondary phases exist. Only one experimental phase diagram each for the sulphide and selenide kesterite system has been published so far [83,84]. In these phase diagrams, a small existence region of single phase kesterite is predicted, with 1–2% (absolute) deviation in the composition at most at growth temperatures around 550°C. In the contrary, the phase diagram of chalcopyrites allows for Cu deficiency of 4% absolute at the growth temperature [85]. This difference is reproduced by equilibrium calculations. Determination of the stability region based on total energy calculations can be compared for chalcopyrites and kesterites. Under Cu-rich conditions, the stability region of Cu_2ZnSnS_4 extends over an area in the chemical potential μ_{Sn}–μ_{Zn} diagram which is about 1 eV long and 0.1 eV wide [68,69,71]. Whereas the stability region of $CuInSe_2$ is about 1 eV long but 0.5 eV wide [86]. So, from the available measurements and calculations, it can be concluded that the existence region of single phase kesterite is smaller compared with chalcopyrites.

Best solar cells have been prepared with a Zn-rich and Cu-poor composition. According to the experimental and calculated phase diagrams, this means that the most likely secondary phase is ZnS(e). It is actually found in $Cu_2ZnSnSe_4$ films [6,48]. ZnS(e) has a wide band gap and usually not an extremely high conductivity, thus it would not harm the open-circuit voltage of the solar cell. It could, however be responsible for the high series resistance observed in all solar cells [5,6]. One can speculate that other secondary phases such as Sn or Cu sulphides or selenides or Cu-Sn sulphide or selenide ternary phases are more detrimental to the solar cells, because of their lower band gap, which reduces the open-circuit voltage, or because of their high conductivity, which could decrease the shunt resistance.

6. SUMMARY OF CHALLENGES

So far solar cell efficiencies of 10% have been achieved with these new materials [4]. For kesterite solar cells to present a commercially viable solution it will certainly be necessary to reach 15% efficiency. Because of the potential negative role of secondary phases, one of the major challenges for these solar cells is the growth of single phase material, particularly because it is very hard to clearly detect secondary phases [53,87]. Even if pure $Cu_2ZnSn(S,Se)_4$ is grown successfully, the control of the structural phases remains a challenge. It will be essential to grow pure kesterite phase, without any admixture of the stannite structure, because of the lower band gap of the stannite. Another challenge for the solar cells is certainly the choice of the correct contact materials. The interface properties are not discussed in this review because information is scarce, and experimental [88] and theoretical [71] data contradict. The control of recombination and doping will depend on the control of the native defects. However in chalcopyrites, the physicochemical nature of the doping defects is still not known [74] and optimisation of solar cells has been quite empirical. A similar approach might work for kesterite solar cells; however because the existence region is smaller than in the chalcopyrites, a better knowledge of the doping defects is desirable.

ACKNOWLEDGEMENTS

Some of the experimental results in this review are published for the first time. We would like to thank the colleagues who provided the samples for these measurements: Björn Schubert from HZB and Dominik Berg from LPV for providing the thin films in Figure 2 and Alexander Nateprov of Institute of Applied Physics, National Academy of Sciences Moldova for the selenide single crystal no. 1.

REFERENCES

1. Green MA, Emery K, Hishikawa Y, Warta W. Solar cell efficiency tables (version 37). *Progress in Photovoltaics* 2011; **19**: 84.
2. Green MA. Estimates of Te and In prices from direct mining of known ores. *Progress in Photovoltaics: Research and Application* 2009; **17**: 347.
3. Schorr S. Structural aspects of adamantine like multinary chalcogenides. *Thin Solid Films* 2007; **515**: 5985.
4. Barkhouse DAR, Gunawan O, Gokmen T, Todorov TK, Mitzi DB. Device characteristics of a 10.1% hydrazine-processed $Cu_2ZnSn(Se,S)_4$ solar cell. *Progress in Photovoltaics: Research and Applications* 2011; in press, doi: 10.1002/pip.1160
5. Mitzi D, Gunawan O, Todorov T, Wang K, Guha S. The path towards a high-performance solution-processed kesterite solar cell. *Solar Energy Materials & Solar Cells* 2011; **95**: 1421.
6. Redinger A, Berg DM, Dale PJ, Djemour R, Gütay L, Eisenbarth T, Valle N, Siebentritt S. Route towards high efficiency single phase $Cu_2ZnSn(S,Se)_4$ thin film solar cells: model experiments and literature review. *Journal of Photovoltaics* 2011; accepted.
7. Hall SR, Szymanski JT, Stewart JM. Kesterite, $Cu_2(Zn,Fe)SnS_4$, and stannite, $Cu_2(Fe,Zn)SnS_4$ structurally similar but distinct minerals. *The Canadian Mineralogist* 1978; **16**: 131.
8. Bernardini GP, Borrini D, Caneschi A, Di Benedetto F, Gatteschi D, Ristori S, Romanelli M. EPR and SQUID magnetometry study of Cu_2FeSnS_4 (stannite) and Cu_2ZnSnS_4 (kesterite). *Physics and Chemistry of Minerals* 2000; **27**: 453.
9. Di Benedetto F, Bernardini GP, Borrini D, Lottermoser W, Tippelt G, Amthauer G. Fe-57- and Sn-119-Mossbauer study on stannite (Cu2FeSnS4)-kesterite (Cu2ZnSnS4) solid solution. *Physics and Chemistry of Minerals* 2005; **31**: 683.
10. Friedlmeier TM, Wieser N, Walter T, Dittrich H, Schock HW. In 14th European Photovoltaic Solar Energy Conference (Stephens and Asc., Barcelona, 1997), Vol. 1, p. 1242.
11. Babu GS, Kishore Kumar YB, Uday Bhaskar P, Sundara Raja V. Effect of post-deposition annealing on the growth of $Cu_2ZnSnSe_4$ thin films for a solar cell absorber layer. *Semiconductor Science and Technology* 2008; **23**: 085023.
12. Schorr S. The crystal structure of kesterite type compounds: a neutron and X-ray diffraction study. *Solar Energy Materials and Solar Cells* 2011; **95**: 1482.
13. Alvarez-Garcia J, Perez-Rodriguez A, Barcones B, Romano-Rodriguez A, Morante JR, Janotti A, Wei S-H, Scheer R. Polymorphism in $CuInS_2$ epilayers: the origin of additional Raman modes. *Applied Physics Letters* 2002; **80**: 562.
14. Su DS, Neumann W, Hunger R, Schubert-Bischoff P, Giersig M, Lewerenz HJ, Scheer R, Zeitler E. CuAu-type ordering in epitaxial $CuInS_2$ films. *Applied Physics Letters* 1998; **73**: 785.
15. Wei SH, Zhang SB, Zunger A. Band structure and stability of zinc-blende-based semiconductor polytypes. *Physical Review B* 1999; **59**: 2478.
16. Neisser A, Hengel I, Klenk R, Matthes TW, Àlvarez-García J, Pérez-Rodríguez A, Romano-Rodríguez A, Lux-Steiner MC. Effect of Ga incorporation in sequentially prepared $CuInS_2$ thin film absorbers. *Solar Energy Materials and Solar Cells* 2001; **67**: 97.
17. Raulot JM, Domain C, Guillemoles JF. Ab initio investigation of potential indium and gallium free chalcopyrite compounds for photovoltaic application. *Journal of Physics and Chemistry of Solids* 2005; **66**: 2019.
18. Chen S, Gong XG, Walsh A, Wei S-H. Crystal and electronic band structure of Cu_2ZnSnX_4 (X = S and Se) photovoltaic absorbers: first-principles insights. *Applied Physics Letters* 2009; **94**: 041903.
19. Paier J, Asahi R, Nagoya A, Kresse G. Cu_2ZnSnS_4 as a potential photovoltaic material: a hybrid Hartree-Fock density functional theory study. *Physical Review B* 2009; **79**: 115126.
20. Persson C. Electronic and optical properties of Cu_2ZnSnS_4 and $Cu_2ZnSnSe_4$. *Journal of Applied Physics* 2010; **107**: 053710.
21. Shay JL Wernick JH, *Ternary Chalcopyrite Semiconductors: Growth, Electronic Properties, and Application*. Pergamon Press: Oxford, 1975.
22. Alonso MI, Garriga M, Rincon CAD, Hernandez E, Leon M. Optical functions of chalcopyrite $CuGaxIn_{1-x}Se_2$ alloys. *Applied Physics A* 2002; **74**: 659.
23. Hönes K, Eickenberg M, Siebentritt S, Persson C. Polarization of defect related optical transitions in chalcopyrites. *Applied Physics Letters* 2008; **93**: 092102.
24. Persson C. Anisotropic hole-mass tensor of $CuIn_{1-x}Ga_x(S,Se)_2$: presence of free carriers narrows the energy gap. *Applied Physics Letters* 2008; **93**: 072106.
25. Schorr S, Hoebler HJ, Tovar M. A neutron diffraction study of the stannite-kesterite solid solution series. *European Journal Of Mineralogy* 2007; **19**: 65.
26. Schubert BA, Marsen B, Cinque S, Unold T, Klenk R, Schorr S, Schock HW. Cu_2ZnSnS_4 thin film solar cells by fast coevaporation. *Progress in Photovoltaics: Research and Applications* 2011; **19**: 93.
27. Redinger A, Berg DM, Dale PJ, Siebentritt S. The consequences of kesterite equilibria for efficient solar cells. *Journal of the American Chemical Society* 2011; **133**: 3320.
28. Williamson WH, Hall WH. X-ray line broadening from filed aluminium and wolfram. *Acta Metallurgica* 1953; **1**: 22.
29. Wyckoff RWG. *The Analytical Expression of the Results of the Theory of Space Groups*. Washington: Carnegie Institution of Washington, 1922.
30. Seol JS, Lee SY, Lee JC, Nam HD, Kim KH. Electrical and optical properties of Cu_2ZnSnS_4 thin films prepared by RF magnetron sputtering process. *Solar Energy Materials and Solar Cells* 2003; **75**: 155.

31. Tanaka T, Nagatomo T, Kawasaki D, Nishio M, Guo QX, Wakahara A, Yoshida A, Ogawa H. Preparation of Cu_2ZnSnS_4 thin films by hybrid sputtering. *Journal of Physics and Chemistry of Solids* 2005; **66**: 1978.
32. Moriya K, Watabe J, Tanaka K, Uchiki H. Characterisation of Cu2ZnSnS4 thin films prepared by photochemical deposition. *Physica Status Solidi C* 2006; **3**: 2848.
33. Scragg JJ, Dale PJ, Peter LM. Towards sustainable materials for solar energy conversion: preparation and photoelectrochemical characterization of Cu_2ZnSnS_4. *Electrochemistry Communications* 2008; **10**: 639.
34. Kamoun N, Bouzouita H, Rezig B. Fabrication and characterization of Cu_2ZnSnS_4 thin films deposited by spray pyrolysis technique. *Thin Solid Films* 2007; **515**: 5949.
35. Sekiguchi K, Tanaka K, Moriya K, Uchiki H. Epitaxial growth of Cu_2ZnSnS_4 thin films by pulsed laser deposition. *Physica Status Solidi C* 2006; **3**: 2618.
36. Zhang J, Shao LX, Fu YJ, Xie EQ. Cu_2ZnSnS_4 thin films prepared by sulfurization of ion beam sputtered precursor and their electrical and optical properties. *Rare Metals* 2006; **25**: 315.
37. Matsushita H, Maeda T, Katsui A, Takizawa T. Thermal analysis and synthesis from the melts of Cu-based quaternary compounds Cu-III-IV-VI, and Cu-2-II-IV-VI4 (II = Zn, Cd; III = Ga, In; IV = Ge, Sn; VI = Se). *Journal of Crystal Growth* 2000; **208**: 416.
38. Wibowo RA, Kim WS, Lee ES, Munir B, Kim KH. Single step preparation of quaternary $Cu_2ZnSnSe_4$ thin films by RF magnetron sputtering from binary chalcogenide targets. *Journal of Physics and Chemistry of Solids* 2007; **68**: 1908.
39. Wibowo RA, Lee ES, Munir B, Kim KH. Pulsed laser deposition of quaternary $Cu_2ZnSnSe_4$ thin films. *Physica Status Solidi A* 2007; **204**: 3373.
40. Altosaar M, Raudoja J, Timmo K, Danilson M, Grossberg M, Krustok J, Mellikov E. $Cu_2Zn_{1-x}Cd_xSn(Se_{1-y}S_y)_4$ solid solutions as absorber materials for solar cells. *Physica Status Solidi A* 2008; **205**: 167.
41. Todorov T, Reuter K, Mitzi DB. High-efficiency solar cell with earth-abundant liquid-processed absorber. *Advanced Materials* 2010; **22**: E156.
42. Ahn S, Jung S, Gwak J, Cho A, Shin K, Yoon K, Park D, Cheong H, Yun JH. Determination of band gap energy (E-g) of Cu2ZnSnSe4 thin films: on the discrepancies of reported band gap values. *Applied Physics Letters* 2010; **97**: 021905.
43. Botti S, Kammerlander D, Marques MAL. Band structures of Cu_2ZnSnS_4 and $Cu_2ZnSnSe_4$ from many-body methods. *Applied Physics Letters* 2011; **98**: 241915.
44. Mortazavi Amiri NB, Postnikov A. Electronic structure and lattice dynamics in kesterite-type $Cu_2ZnSnSe_4$ from first-principles calculations. *Physical Review B* 2010; **82**: 205204.
45. Siebentritt S. In *Wide Gap Chalcopyrites*. Siebentritt S, Rau U (eds). Springer: Berlin, Heidelberg, New York, 2006, 113.
46. Larsen J, Gütay L, Siebentritt S. In 37th IEEE Photovoltaic Specialist Conference. IEEE, Seattle, 2011.
47. Grossberg M, Krustok J, Timmo K, Altosaar M. Radiative recombination in $Cu_2ZnSnSe_4$ monograins studied by photoluminescence spectroscopy. *Thin Solid Films* 2009; **517**: 2489.
48. Redinger A, Hönes K, Fontané X, Izquierdo-Roca V, Saucedo E, Valle N, Pérez-Rodríguez A, Siebentritt S. Detection of a ZnSe secondary phase in coevaporated $Cu_2ZnSnSe_4$ thin films. *Applied Physics Letters* 2011; **98**: 101907.
49. Miyamoto Y, Tanaka K, Oonuki M, Moritake N, Uchiki H. Optical properties of Cu2ZnSnS4 thin films prepared by sol–gel and sulfurization method. *Japanese Journal of Applied Physics* 2008; **47**: 596.
50. Unold T, Kretzschmar S, Just J, Zander O, Schubert B, Marsen B, Schock H-W. In 37th IEEE Photovoltaic Specialist Conference. IEEE, Seattle, 2011.
51. Leitao JP, Santos NM, Fernandes PA, Salome PMP, da Cunha AF, Gonzalez JC, Ribeiro GM, Matinaga FM. Photoluminescence and electrical study of fluctuating potentials in Cu(2)ZnSnS(4)-based thin films. *Physical Review B* 2011; **84**: 024120.
52. Tanaka K, Miyamoto Y, Uchiki H, Nakazawa K, Araki H. Donor-acceptor pair recombination luminescence from Cu_2ZnSnS_4 bulk single crystals. *Physica Status Solidi A-Applications and Materials Science* 2006; **203**: 2891.
53. Dale PJ, Hoenes K, Scragg JJ, Siebentritt S. In 34th IEEE Photovoltaic Specialist Conference. IEEE, Philadelphia, 2009; 1956.
54. Katagiri H, Jimbo K, Yamada S, Kamimura T, Shwe Maw W, Fukano T, Ito T, Motohiro T. Enhanced conversion efficiencies of Cu_2ZnSnS_4-based thin film solar cells by using preferential etching technique. *Applied Physics Express* 2008; **1**: 041201.
55. Guo Q, Ford GM, Yang W-C, Walker BC, Stach EA, Hillhouse HW, Agrawal R. Fabrication of 7.2% efficient CZTSSe solar cells using CZTS nanocrystals. *Journal of the American Chemical Society* 2010; **132**: 17384.
56. Repins I, Vora N, Beall C, Wei SH, Yan Y, Romero MJ, Teeter G, Du H, To B, Young M, Noufi R. Kesterite and chalcopyrites: a comparison of close cousins. *Materials Research Society Symposium Proceedings* 2011; **1324**: d17–01.
57. Rau U, Werner J. Radiative efficiency limits of solar cells with lateral band-gap fluctuations. *Applied Physics Letters* 2004; **84**: 3735.
58. Guen L, Glaunsinger WS. Electrical, magnetic and EPR studies of the quaternary chalcogenides $Cu_2A^{II}B^{IV}X_4$ prepared by iodine transport. *Journal of Solid State Chemistry* 1980; **35**: 10.
59. Birkholz M, Kanschat P, Weiss T, Czerwensky M, Lips K. Low-temperature EPR study of extrinsic and intrinsic defects in CuGaSe2. *Physical Review B* 1999; **59**: 12268.

60. Nishi T, Medvedkin GA, Katsumata Y, Sato K, Miyake H. Electron paramagnetic resonance and photoluminescence study of defects in CuGaSe2 single crystals grown by travelling heater method. *The Japanese Journal of Applied Physics* 2001; **40**: 59.
61. Aubin V, Binet L, Guillemoles JF. Electron spin resonance studies of Cu(In,Ga)Se thin films. *Thin Solid Films* 2003; **431–2**: 167.
62. Hoenes K, Zscherpel E, Scragg JJ, Siebentritt S. Shallow defects in Cu_2ZnSnS_4. *Physica B: Condensed Matter* 2009; **404**: 4949.
63. Oishi K, Saito K, Ebina K, Nagahashi M, Jimbo K, Maw WS, Katagiri H, Yamazaki M, Araki H, Takeuchi A. Growth of Cu_2ZnSnS_4 thin films on Si (100) substrates by multisource evaporation. *Thin Solid Films* 2008; **517**: 1449.
64. Luckert F, Hamilton DI, Yakushev MV, Beattie NS, Zoppi G, Moynihan M, Forbes I, Karotki AV, Mudryi AV, Grossberg M, Krustok J, Martin RW. Optical properties of high quality $Cu_2ZnSnSe_4$ thin films. *Applied Physics Letters* 2011; **99**: 062104.
65. Dirnstorfer I, Wagner M, Hofmann DM, Lampert MD, Karg F, Meyer BK. Characterization of CuIn(Ga)Se2 thin films III In-rich layers. *Physica Status Solidi A* 1998; **168**: 163.
66. Bauknecht A, Siebentritt S, Albert J, Lux-Steiner MC. Radiative recombination via intrinsic defects in $CuGaSe_2$. *Journal of Applied Physics* 2001; **89**: 4391.
67. Siebentritt S, Rega N, Zajogin A, Lux-Steiner MC. In Conference on Photo-responsive Materials (Phys. Stat. Sol. C 1(9)). Leitch AWR, Botha R. (eds). Wiley, Kariega Game Reserve, South Africa, 2004; 2304.
68. Chen SY, Gong XG, Walsh A, Wei SH. Defect physics of the kesterite thin-film solar cell absorber Cu2ZnSnS4. *Applied Physics Letters* 2010; **96**: 021902.
69. Nagoya A, Asahi R, Wahl R, Kresse G. Defect formation and phase stability of Cu_2ZnSnS_4 photovoltaic material. *Physical Review B* 2010; **81**: 113202.
70. Biswas K, Lany S, Zunger A. The electronic consequences of multivalent elements in inorganic solar absorbers: multivalency of Sn in Cu[sub 2]ZnSnS [sub 4]. *Applied Physics Letters* 2010; **96**: 201902.
71. Chen S, Yang J-H, Gong XG, Walsh A, Wei S-H. Intrinsic point defects and complexes in the quaternary kesterite semiconductor Cu_{2}ZnSnS_{4}. *Physical Review B* 2010; **81**: 245204.
72. Maeda T, Nakamura S, Wada T. First-principles calculations of vacancy formation in In-free photovoltaic semiconductor Cu2ZnSnSe4. *Thin Solid Films* 2011; **519**: 7513.
73. Maeda T, Nakamura S, Wada T. First principles calculations of defect formation in In-free photovoltaic semiconductors Cu_2ZnSnS_4 and $Cu_2ZnSnSe_4$. *Japanese Journal of Applied Physics* 2011; **50**: 04DP07.
74. Siebentritt S, Igalson M, Persson C, Lany S. The electronic structure of chalcopyrites—bands, point defects and grain boundaries. *Progress in Photovoltaics: Research and Applications* 2010; **18**: 390.
75. Nagoya A, Asahi R, Kresse G. First-principles study of Cu_2ZnSnS_4 and the related band offsets for photovoltaic applications. *Journal of Physics: Condensed Matter* 2011; **23**: 404203.
76. Ito K, Nakazawa T. Electrical and optical properties of stannite-type quaternary semiconductor thin films. *Japanese Journal of Applied Physics* 1988; **27**: 2094.
77. Nakayama N, Ito K. Sprayed films of stannite Cu2ZnSnS4. *Applied Surface Science* 1996; **92**: 171.
78. Katagiri H, Sasaguchi N, Hando S, Hoshino S, Ohashi J, Yokota T. Preparation and evaluation of Cu_2ZnSnS_4 thin films by sulfurization of E-B evaporated precursors. *Solar Energy Materials and Solar Cells* 1997; **49**: 407.
79. Katagiri H, Saitoh K, Washio T, Shinohara H, Kurumadani T, Miyajima S. Development of thin film solar cell based on Cu_2ZnSnS_4 thin films. *Solar Energy Materials and Solar Cells* 2001; **65**: 141.
80. Katagiri H, Ishigaki N, Ishida T, Saito K. Characterization of Cu_2ZnSnS_4 thin films prepared by vapor phase sulfurization. *Japanese Journal of Applied Physics Part 1-Regular Papers Short Notes & Review Papers* 2001; **40**: 500.
81. Friedlmeier TM, Dittrich H, Schock HW. In 11th International Conference on Ternary and Multinary Compounds. ICTMC-11 Institute of Physics Publishing, Salford, UK, 1998.
82. Romero MJ, Du H, Teeter G, Yan Y, Al-Jassim MM. Comparative study of the luminescence and intrinsic point defects in the kesterite Cu_2ZnSnS_4 and chalcopyrite $Cu(In,Ga)Se_2$ thin films used in photovoltaic applications. *Physical Review B* 2011; **84**: 165324.
83. Dudchak IV, Piskach LV. Phase equilibria in the Cu_2SnSe_3–$SnSe_2$–ZnSe system. *Journal of Alloys and Compounds* 2003; **351**: 145.
84. Olekseyuk ID, Dudchak IV, Piskach LV. Phase equilibria in the Cu_2S-ZnS-SnS_2 system. *Journal of Alloys and Compounds* 2004; **368**: 135.
85. Gödecke T, Haalboom T, Ernst F. Phase equilibria of Cu-In-Se I: stable states and nonequilibrium states of the In_2Se_3-Cu_2Se subsystem. *Zeitschrift für Metallkunde* 2000; **91**: 622.
86. Persson C, Lany S, Zhao Y-J, Zunger A. n-type doping of $CuInSe_2$ and $CuGaSe_2$. *Physical Review B* 2005; **72**: 035211.
87. Fontané X, Calvo-Barrio L, Izquierdo-Roca V, Saucedo E, Pérez-Rodriguez A, Morante JR, Berg DM, Dale PJ, Siebentritt S. In-depth resolved Raman scattering analysis of electrodeposited Cu_2ZnSnS_4 layers for solar cell applications: identification of secondary phases. In press 2011.
88. Haight R, Barkhouse A, Gunawan O, Shin S, Copel M, Hopstaken M, Mitzi CB. Band alignment at the $Cu_2ZnSn(S_xSe_{1-x})_4$/CdS interface. *Applied Physics Letters* 2011; **98**: 253502.